

Pen-on-Paper Flexible Electronics

Analisa Russo, Bok Yeop Ahn, Jacob J. Adams, Eric B. Duoss, Jennifer T. Bernhard, and Jennifer A. Lewis*

Printed electronics constitute an emerging class of materials with potential application in photovoltaics,^[1] transistors,^[2,3] displays,^[4–6] batteries,^[7] antennas,^[8] and sensors.^[9,10] Recent attention has focused on paper substrates as a low-cost, enabling platform for flexible, lightweight, and disposable devices.^[11–13] Such devices require conductive electrodes, which, to date, have been deposited by sputter coating,^[14] inkjet printing,^[15] and airbrush spraying.^[11] However, these deposition methods are either costly or employ dilute inks that readily permeate the paper substrate. Here, we demonstrate a facile pen-on-paper approach for creating flexible printed electronics. Using a rollerball pen filled with conductive silver ink, we directly write conductive text, electronic art, interconnects for light emitting diode (LED) arrays, and three-dimensional (3D) antennas on paper.

Paper substrates offer many advantages for printed electronic devices. Not only is paper widely available and inexpensive, it is lightweight, biodegradable, and can be rolled or folded into 3D configurations. Functional electronic components, including thermochromic displays,^[14] disposable radio frequency identification (RFID) tags,^[16,17] and cellulose-based batteries,^[18] have recently been produced on paper substrates. The wide variety of available paper textures, compositions, and coatings can be exploited to enable specific device architectures. For example, highly absorbent paper is suitable for disposable microfluidic and diagnostic devices,^[19] whereas smooth photo-quality paper is used for coloured electrowetting pixels.^[20] Facile routes to creating devices “on-the-fly” under ambient conditions are needed to fully exploit the potential of paper-based printed electronics.

A. Russo,^[+] Dr. B. Y. Ahn,^[+] Dr. E. B. Duoss,^[+] Prof. J. A. Lewis
Department of Materials Science and Engineering
University of Illinois at Urbana-Champaign
Urbana, IL 61801, USA
E-mail: jalewis@illinois.edu

Prof. J. A. Lewis
Department of Chemical and Biomolecular Engineering
University of Illinois at Urbana-Champaign
Urbana, IL 61801, USA

Dr. J. J. Adams, Prof. J. T. Bernhard
Electromagnetics Laboratory
Department of Electrical and Computer Engineering
University of Illinois at Urbana-Champaign
Urbana, IL 61801, USA

[+] Present address: Center for Micro- and Nanotechnology, Lawrence Livermore National Laboratory, Livermore, CA 94551, USA

[++] A.R. and B.Y.A. contributed equally to this work.

DOI: 10.1002/adma.201101328

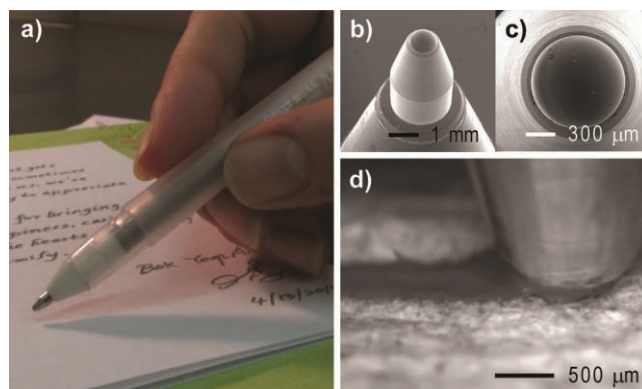


Figure 1. a) Optical image of a rollerball pen loaded with a conductive silver ink. The background shows conductive text written on Xerox paper. b and c) SEM images of the side and top views of the rollerball pen. d) Optical image of the rollerball pen tip, captured during writing a conductive silver track on a Xerox paper.

The pen-on-paper (PoP) paradigm offers a unique approach to fabricating flexible devices by using a patterning instrument that is itself as ubiquitous and portable as the paper substrate. Rollerball pens are especially well suited for dispensing conductive inks due to their compatibility with liquids and gels.^[21] Pens with ball diameters ranging from 250 μm to nearly a millimeter are commercially available and are specifically engineered for precision writing on paper. **Figure 1a–c** shows a representative rollerball pen with a ball diameter (d) of 960 μm that is filled with colloidal silver ink for writing conductive features on Xerox paper. In this example, conductive text is printed with features that are approximately 650 μm wide (**Figure 1d**).

Central to the PoP approach is the design of a silver ink that readily flows through the rollerball pen tip during writing, does not leak from, dry out, or coagulate within the pen, and is conductive upon printing under ambient conditions. To create an ink with these attributes, we synthesized silver particles in an aqueous solution by reducing silver nitrate in the presence of a surface capping agent, poly(acrylic acid) (PAA) and diethanolamine.^[22–26] Using a multistep procedure, we first mixed these components to create a population of silver nanoparticles (~5 nm in diameter). This particle population is then ripened by heating the solution to 65 $^{\circ}\text{C}$ for 1.5 h to yield a mean diameter of 400 ± 120 nm, as shown in **Figure 2a**. Ethanol, a poor solvent for the PAA-coated particles, is added to induce rapid coagulation and then the precipitate is centrifuged to achieve high solids loading. The silver particles are redispersed in water

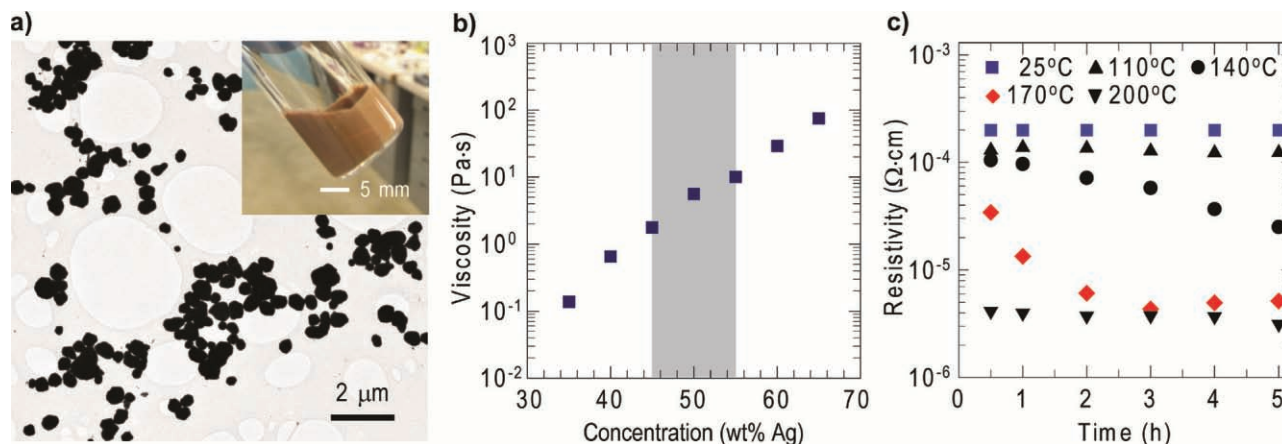


Figure 2. a) TEM image of the synthesized silver particles and optical image of a representative ink (inset). b) Apparent ink viscosity (η) measured at 1 s^{-1} as a function of silver content. The shaded region indicates optimal ink formulations for printing using a $960 \mu\text{m}$ diameter rollerball tip. c) Electrical resistivity of the silver inks (50 wt% silver) as-printed at $25 \text{ }^\circ\text{C}$ and as a function of annealing temperature and time.

to remove the PAA capping agent, which is initially present at 10% by weight of silver, and again concentrated by centrifugation. This process is repeated three times, resulting in complete removal of PAA (see Supporting Information, Figure S1). Finally, hydroxyethyl cellulose (HEC), a viscosifier, is added to tailor the ink rheology.

Figure 2b shows the apparent viscosity (η) acquired at a shear rate of 1 s^{-1} as a function of solids loading for silver inks prepared with an HEC:Ag ratio of 3 wt%. The apparent viscosity is $\sim 0.3 \text{ Pa}\cdot\text{s}$ for the inks containing 35 wt% silver particles. However, the viscosity increases by three orders of magnitude for inks composed of 65 wt% silver particles. Over this compositional range, each ink exhibits shear thinning behavior, which is most pronounced at the highest solids loading (see Supporting Information, Figure S2). Of these compositions, only those inks with 45–55 wt% silver particles and, hence, viscosities of 1–10 $\text{Pa}\cdot\text{s}$ reliably flow through the ballpoint tip without leaking, skipping, or clogging. Notably, these inks are stable for months when stored in properly sealed containers and can flow through rollerball pens with diameters as small as $250 \mu\text{m}$ (see Supporting Information, Figure S3). In addition, these inks can be written on both soft and rigid substrates, including polymer films, wood, and ceramics by this PoP approach (see Supporting Information, Figure S4).

Figure 2c shows the electrical resistivity of the silver ink (50 wt% silver) after printing and drying under ambient conditions ($25 \text{ }^\circ\text{C}$) and as a function of annealing temperature and time. To precisely control the sample dimensions, silver films ($1 \text{ cm} \times 1 \text{ cm}$ wide, $12 \mu\text{m}$ in height) are formed by doctor blading the ink on a glass substrate. The ink is conductive after drying at room temperature for 30 min, exhibiting an electrical resistivity of $1.99 \times 10^{-4} \Omega\cdot\text{cm}$. Upon annealing at $110 \text{ }^\circ\text{C}$, a slight decrease in resistivity is observed likely due to evaporation of residual solvent. Annealing to higher temperatures ($\geq 170 \text{ }^\circ\text{C}$) results in a significant decrease in the electrical resistivity ($4.34 \times 10^{-6} \Omega\cdot\text{cm}$) as particle sintering ensues. Corresponding images of the microstructural evolution observed during annealing are provided as the supplementary information (Figure S5). Importantly, the printed inks exhibit an electrical resistivity that is

several orders of magnitude below that observed for silver nanoparticle inks (mean diameter = $20 \pm 5 \text{ nm}$) previously developed for omnidirectional printing of flexible, stretchable, and spanning electrodes.^[22] Their greatly enhanced electrical performance likely arises due to removal of the PAA capping layer from the silver particle surfaces as well as their larger mean particle size. This ability to directly write conductive features under ambient conditions is essential for the PoP approach.

To investigate the mechanical flexibility of the printed features, we produced a linear array of 5 silver electrodes (width = $620 \mu\text{m}$, height = $\sim 20 \mu\text{m}$, and length = 1.5 cm) spaced 1.5 mm apart using a $960 \mu\text{m}$ roller ball pen filled with colloidal silver ink (50 wt% silver) on Xerox paper and dried at room temperature for 24 h in air. The silver ink conformally coats the fibrous paper surface, exhibiting good adhesion as confirmed by the ASTM D3330 tape test. The electrode-patterned paper substrates are actuated between the flat and bent states at a bending rate of 2 cm s^{-1} to a specified minimum bend radius using a custom-built mechanical stage coupled to a computer-controlled 3-axis micropositioning system (see Supporting Information, Figure S6). Optical images of the test specimens at minimum bend radii (r) of 2.9 mm , 1.6 mm , and 0.5 mm are shown in Figure 3a. Corresponding scanning electron images reveal that there is no noticeable crack formation or delamination during the first bend cycle (Figure 3b). We measured the electrical resistance (R) as a function of bend radius and number of bend cycles, and average R values obtained from the five electrodes are reported in Figure 3d. For r of 2.9 mm and 1.6 mm , the silver electrodes exhibit a robust response over 10 000 bending cycles with a slight increase in their respective electrical resistance of 1.2 and 1.6 relative to their initial, as-printed state. For the most extreme bend radius of 0.5 mm , the electrical resistance increases gradually after many cycles. Two electrodes undergo cracking and fail after 6000 cycles, while three electrodes survive after 10 000 cycles exhibiting a 3.2-fold increase in their electrical resistance relative to their initial, as-printed state. After 10 000 cycles at a bend radius of 0.5 mm , their microstructure is observed by SEM in both flat (top) and bent configurations, with bend radii of 1.6 mm

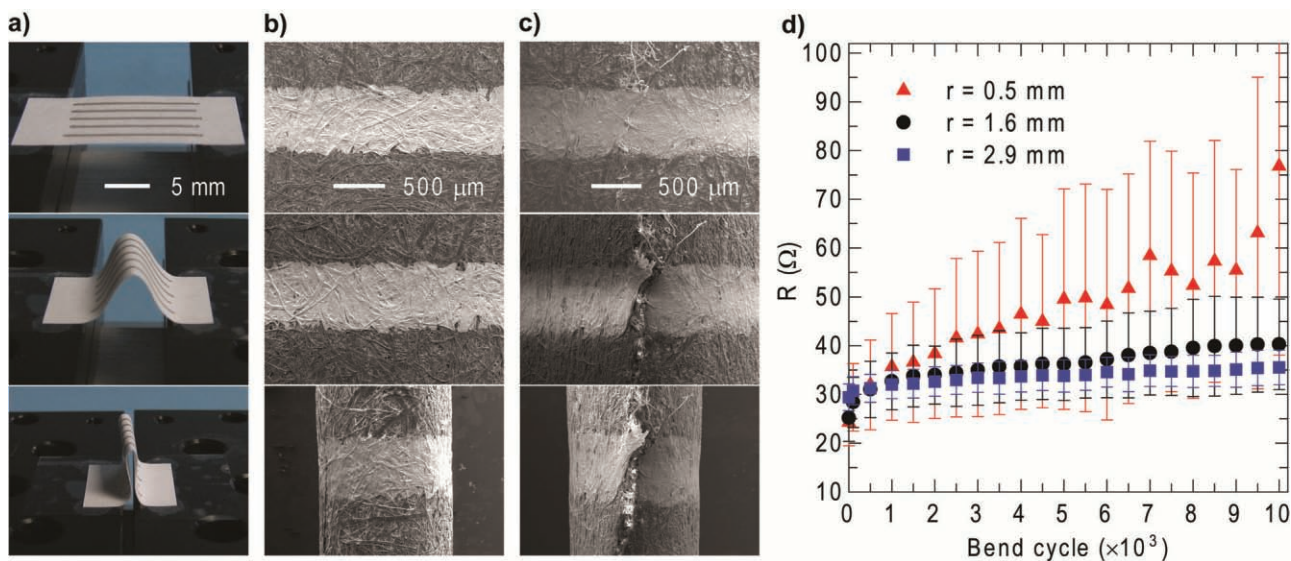


Figure 3. a) Optical images of silver electrode arrays in flat (top) and bent states with bend radii of 1.6 mm (middle), 0.5 mm (bottom). b) SEM images of the silver electrodes in flat and bent states before bend cycles. c) SEM images of the silver electrodes in flat and bent states after 10 000 bend cycles. d) Electrical resistance as a function of bend cycle of the printed silver electrodes of varying bend radius.

(middle), 0.5 mm (bottom), respectively (Figure 3c). Repeated fatigue in a nearly folded state ($r = 0.5$ mm) leads to crease formation in the underlying paper substrate in the direction perpendicular to the printed silver electrode(s). Ultimately, cracks can form within the electrodes along this crease. This crease, which is barely visible in the unbent state, is easily observed as r decreases. Notably, upon returning to the unbent state, the conductive pathway along the electrode is restored. The SEM image of the flat specimen reveals the formation of a cold joint between the two crack surfaces.^[27]

To demonstrate the device fabrication capabilities afforded the PoP approach, we produced electronic art, multi-color LED displays, and 3D antennas on paper substrates by using rollerball pens and other office supplies. As a first example, an electronic sketch of the famous painting “Sae-Han-Do” by Jung Hee Kim is drawn using a silver ink-filled rollerball pen (Figure 4a). The yellow-grey background is first printed on Xerox paper using a desktop printer, and then the trees, house, and Chinese characters are hand-drawn. The printed silver features that overlap form a conductive network upon drying under ambient conditions (Figure 4b). The printed feature size is dependent upon writing pressure and speed. Hence, even though the rollerball diameter is 960 μm , the resulting feature sizes range from ~ 300 μm to 1 mm wide. A surface-mount LED (1.25 mm \times 2 mm \times 0.8 mm) is placed in a gap that is left in the rooftop of the house. To form contacts, a drop of concentrated silver ink (65 wt% solids loading Ag) is used as a conductive adhesive (Figure 4c). After drying at room temperature for an hour, this LED is illuminated by using a 5 V battery as a power source and electrical leads located at the indicating arrows.

To demonstrate large-area flexible paper displays, we fabricated a multi-color 25 \times 16 LED array (Figure 4d). First, a series of parallel ground lines with a 4 mm center-to-center spacing are printed on a Xerox paper using a silver ink-filled

rollerball pen. These lines are crossed by strips (1.5 mm wide) of adhesive-backed paper containing single silver electrodes, with additional electrodes hand-drawn, as needed. The surface-mount LEDs are adhered to the display by using a drop of superglue placed on the back of each LED. They are then connected to the printed silver electrodes by depositing a drop of concentrated silver ink (65 wt% solids) at each terminal. A schematic of the interconnect design and magnified optical images of these devices are provided in supplementary information (Figure S7). Although the voltage and current ratings of these LEDs differ by color, they can be integrated into an array powered by a single 9 V battery. As one example, we produce the displayed characters shown in Figure 4d by illuminating a total of 34 LEDs composed of four different colors (9 red, 8 green, 9 blue, and 8 orange).

The PoP approach can also be used for high frequency devices. As an example, we fabricated 3D antennas^[28] for operation in the 1.9 GHz band (Figure 4e). Specifically, the radiating elements composed of eight tapered meanderline arms ($w = 650$ μm , center-to-center spacing = 1 mm) are printed by desktop printer on adhesive-back paper, and then conductive silver traces are hand-drawn on the guide lines using a silver ink-filled rollerball pen. The pattern is then cut to form a pin-wheel structure, which is conformally adhered to the surface of a hollow glass hemisphere (radius = 12.7 mm). The 3D antenna is completed by attaching the patterned hemisphere to a low-loss laminate substrate (Duroid 5880, Rogers Corp.) with copper feedlines. The reflection coefficient of this 3D antenna is measured using a network analyzer. The reflected power quantifies how well energy can be coupled from the transceiver to the antenna and vice-versa.^[29] The measured center frequency is 1.87 GHz with efficiency of 20–30% (Figure 4f), which is significantly lower than that recently achieved by conformal printing conductive features directly onto glass hemispheres. However,

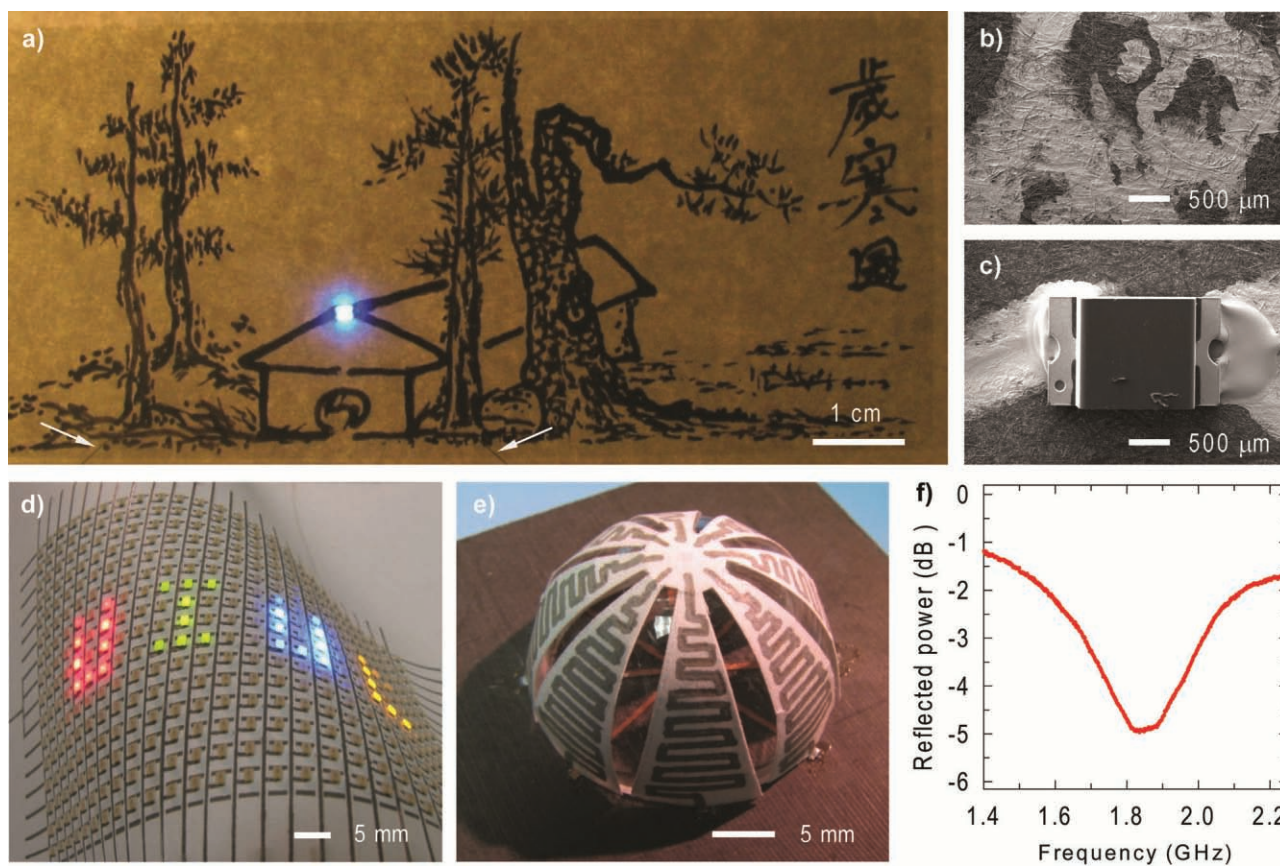


Figure 4. a) Optical image of conductive electronic art drawn by a silver-ink filled rollerball pen on Xerox paper. b) SEM image at the root of the a tree, showing a conductive silver network. c) SEM image of the LED chip, adhered to the paper substrate with the conductive silver interconnects. d) Optical image of a flexible paper display containing a LED array (25 × 16) on a Xerox paper. e) Optical image of the 3D antenna, fabricated by drawing periodic conductive silver tracks on a sticky paper, followed by conformally adhering it to a hemispherical hollow glass substrate. f) Reflected power of the 3D antenna as a function of frequency.

those 3D antennas required heat treatment to 550 °C to obtain silver meanderlines with an electrical resistivity approaching that of bulk silver ($\sim 1.6 \times 10^{-6} \Omega \cdot \text{cm}$).^[28] Although the reflected power of the paper antenna (-4.9 dB at 1.85 GHz) is not ideal, we demonstrate that a functioning antenna can be made by this simple fabrication approach. Further optimization of the ink properties, meanderline, and feedline design is now underway to improve antenna performance.

In summary, this pen-on-paper approach offers a low-cost, portable fabrication route for printed electronic and optoelectronic devices. The ink design strategy described above is quite general. With little effort, it can be extended to other particle-based inks, including those based on oxide, semiconductor, and carbon building blocks. We therefore envision that our PoP approach could be implemented for paper-based batteries, medical diagnostics^[19] and other functional devices.

Supporting Information

Supporting Information is available from the Wiley Online Library or from the author.

Acknowledgements

This material is based upon work supported by the U.S. Department of Energy, Division of Materials Sciences and Engineering under Award No. DEFG-02-07ER46471, through the Frederick Seitz Materials Research Laboratory (FSMRL) at the University of Illinois. We gratefully acknowledge use of the FSMRL Central Facilities, including Center for Microanalysis of Materials.

Received: April 9, 2011
Published online:

- [1] C. N. Hoth, S. A. Choulis, P. Schilinsky, C. J. Brabec, *Adv. Mater.* **2007**, *19*, 3973.
- [2] H. Sirringhaus, T. Kawase, R. H. Friend, T. Shimoda, M. Inbasekaran, W. Wu, E. P. Woo, *Science* **2000**, *290*, 2123.
- [3] H. Okimoto, T. Takenobu, K. Yanagi, Y. Miyata, H. Shimotani, H. Kataura, Y. Iwasa, *Adv. Mat.* **2010**, *22*, 3981.
- [4] B. Comiskey, J. D. Albert, H. Yoshizawa, J. Jacobson, *Nature* **1998**, *394*, 253.
- [5] T. Zyung, S. H. Kim, H. Y. Chu, J. H. Lee, S. C. Lim, J. I. Lee, J. Oh, *Proc. IEEE* **2005**, *93*, 1265.
- [6] Y. Kondo, H. Tanabe, T. Otake, *IEICE Trans. Electron.* **2010**, *E39-C*, 1602.

- [7] L. Hu, J. W. Choi, Y. Yang, S. Jeong, F. L. Mantia, L. F. Cui, Y. Cui, *PNAS* **2009**, *106*, 21490.
- [8] V. Subramanian, J. M. J. Frechet, P. C. Chang, D. C. Huang, J. B. Lee, S. E. Molesa, A. R. Murphy, D. R. Redinger, S. K. Volkman, *Proc. IEEE* **2005**, *93*, 1330.
- [9] S. H. Lim, J. W. Kemling, L. Feng, K. S. Suslick, *Analyst* **2009**, *134*, 2453.
- [10] C. T. Wang, K. Y. Huang, D. T. W. Lin, W. C. Liao, H. W. Lin, Y. C. Hu, *Sensors* **2010**, *10*, 5054.
- [11] A. C. Siegel, S. T. Phillips, M. D. Dickey, N. Lu, Z. Suo, G. M. Whitesides, *Adv. Funct. Mater.* **2010**, *20*, 28.
- [12] A. Rida, L. Yang, R. Vyas, M. M. Tentzeris, *IEEE Antennas Propagation Mag.* **2009**, *51*, 13.
- [13] A. W. Martinez, S. T. Phillips, M. J. Butte, G. M. Whitesides, *Angew. Chem. Int. Ed.* **2007**, *46*, 1318.
- [14] A. C. Siegel, S. T. Phillips, B. J. Wiley, G. M. Whitesides, *Lab Chip* **2009**, *9*, 2775.
- [15] B.-J. de Gans, P. C. Duineveld, U. S. Schubert, *Adv. Mat.* **2004**, *16*, 203.
- [16] M. Dragoman, E. Flahaut, D. Dragoman, M. Al Ahmad, R. Plana, *Nanotechnology* **2009**, *20*, 375203.
- [17] M. Jung, J. Kim, J. Noh, N. Lim, C. Lim, G. Lee, J. Kim, H. Kang, K. Jung, A. D. Leonard, J. M. Tour, G. Cho, *IEEE Trans. Electron. Devices* **2010**, *57*, 571.
- [18] G. Nyström, A. Razaq, M. Stromme, L. Nyholm, A. Mitranyan, *Nano Lett.* **2009**, *9*, 3635.
- [19] A. W. Martinez, S. T. Phillips, B. J. Wiley, M. Gupta, G. M. Whitesides, *Lab Chip* **2008**, *8*, 2146.
- [20] D. Y. Kim, A. J. Steckl, *Appl. Mater. Interfaces.* **2010**, *2*, 3318.
- [21] H. Gostony, S. L. Schneider, *The Incredible Ball Point Pen: A Comprehensive History & Price Guide*, Schiffer Publishing, PA, USA **1998**.
- [22] B. Y. Ahn, E. B. Duoss, M. J. Motala, X. Guo, S.-I. Park, Y. Xiong, J. Yoon, R. G. Nuzzo, J. A. Rogers, J. A. Lewis, *Science* **2009**, *323*, 1590.
- [23] Y. Sun, Y. Xia, *Science* **2002**, *298*, 2176.
- [24] B. Wiley, Y. Sun, Y. Xia, *Acc. Chem. Res.* **2007**, *40*, 1067.
- [25] M. Yamamoto, Y. Kashiwagi, M. Nakamoto, *Langmuir* **2006**, *22*, 8581.
- [26] A. Pyatenko, M. Yamaguchi, M. Suzuki, *J. Phys. Chem. C* **2007**, *111*, 7910.
- [27] S. H. Hur, O. O. Park, J. A. Rogers, *App. Phys. Lett.* **2005**, *86*, 243502.
- [28] J. J. Adams, E. B. Duoss, T. F. Malkowski, M. J. Motala, B. Y. Ahn, R. G. Nuzzo, J. T. Bernhard, J. A. Lewis, *Adv. Mater.* **2011**, *23*, 1335.
- [29] M. Geissler, O. Litschke, D. Heberling, P. Waldow, I. Wolff, *Proc. 2003 IEEE Int. Symp. Antennas Propag.* **2003**, 743.